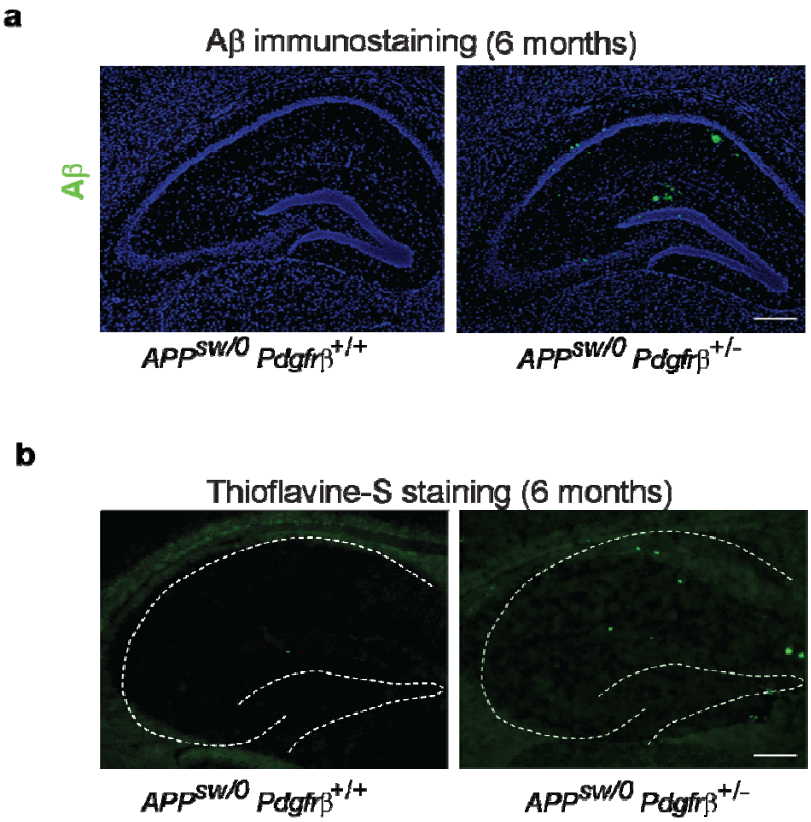

Supplementary Figure S1. Aβ pathology in pericyte-deficient *APP$^{sw/0}$ Pdgfrβ$^{+/-}$* mice. a-b, Representative cortex and hippocampus sections stained for Aβ (**a**) and thioflavin S (**b**) in 6-month old *APP$^{sw/0}$*; *Pdgfrβ$^{+/+}$* and *APP$^{sw/0}$*; *Pdgfrβ$^{+/-}$* mice. Images are representative findings from 6 mice per group. Scale bar, 100 μm.

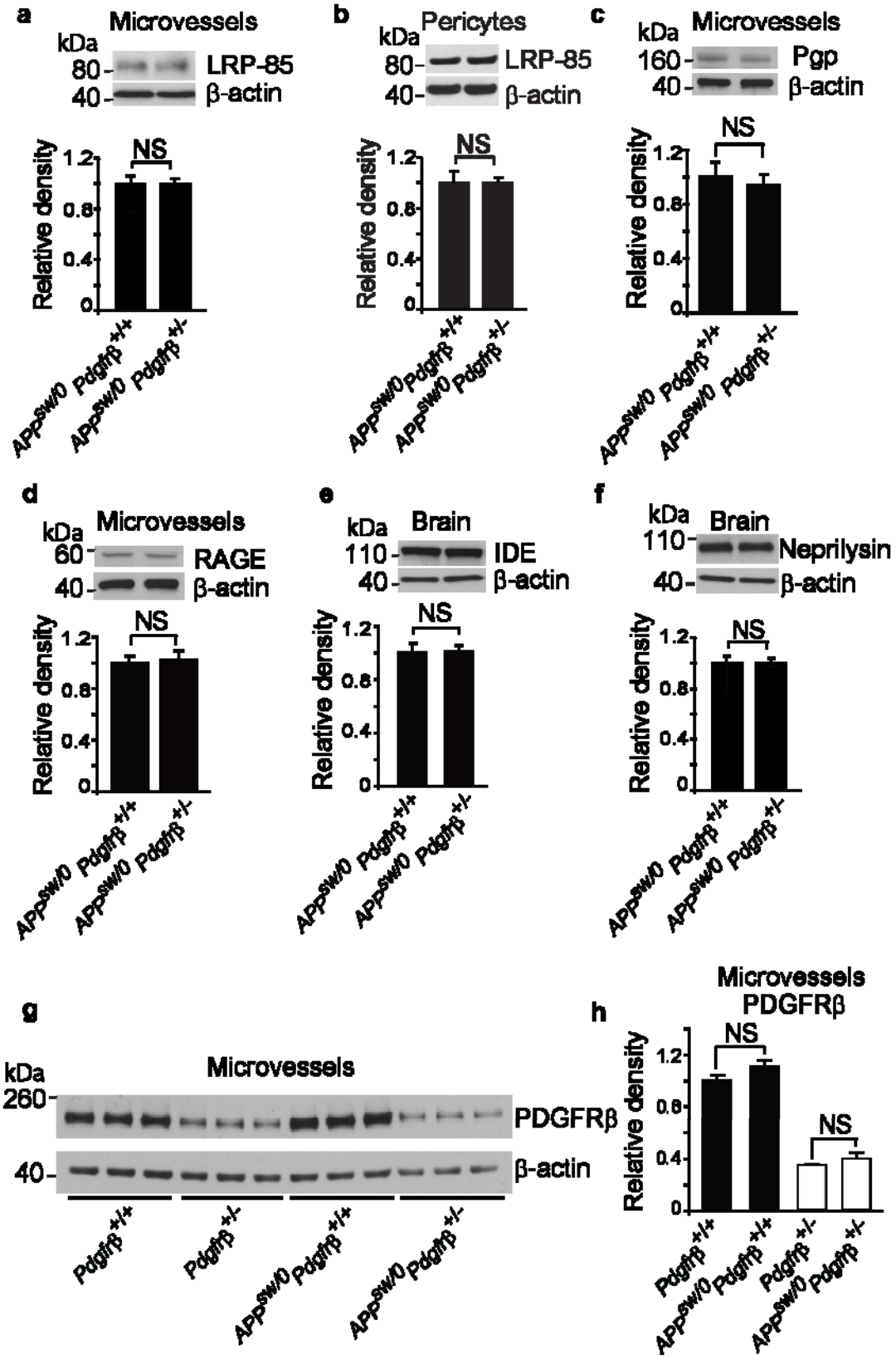
a
Microvessels
kDa
80
40
LRP-85
β-actin
Relative density
NS
1.2
0.8
0.4
0
APPSw/0 Pdgfrβ +/+
APPSw/0 Pdgfrβ +/-
b
Pericytes
kDa
80
40
LRP-85
β-actin
Relative density
NS
1.2
0.8
0.4
0
APPSw/0 Pdgfrβ +/+
APPSw/0 Pdgfrβ +/-
c
Microvessels
kDa
160
40
Pgp
β-actin
Relative density
NS
1.2
0.8
0.4
0
APPSw/0 Pdgfrβ +/+
APPSw/0 Pdgfrβ +/-
d
Microvessels
kDa
60
40
RAGE
β-actin
Relative density
NS
1.2
0.8
0.4
0
APPSw/0 Pdgfrβ +/+
APPSw/0 Pdgfrβ +/-
e
Brain
kDa
110
40
IDE
β-actin
Relative density
NS
1.2
0.8
0.4
0
APPSw/0 Pdgfrβ +/+
APPSw/0 Pdgfrβ +/-
f
Brain
kDa
110
40
Neprilysin
β-actin
Relative density
NS
1.2
0.8
0.4
0
APPSw/0 Pdgfrβ +/+
APPSw/0 Pdgfrβ +/-
g
Microvessels
kDa
260
40
PDGFRβ
β-actin
Pdgfrβ +/+
Pdgfrβ +/-
APPSw/0 Pdgfrβ +/+
APPSw/0 Pdgfrβ +/-
h
Microvessels
PDGFRβ
Relative density
NS
NS
1.2
0.8
0.4
0
Pdgfrβ +/+
APPSw/0 Pdgfrβ +/+
Pdgfrβ +/-
APPSw/0 Pdgfrβ +/-

Supplementary Figure S2. Expression of different Aβ clearance receptors and enzymes and PDGFRβ in pericyte-deficient *APP$^{sw/0}$Pdgfrβ$^{+/-}$* mice. a-b, Relative abundance of LRP1 compared to β-actin determined by immunoblotting of brain microvessels (**a**) and isolated pericytes (**b**) from 9 month old *APP$^{sw/0}$ Pdgfrβ$^{+/+}$* and *APP$^{sw/0}$*; *Pdgfrβ$^{+/-}$* littermates. **c-d**, Relative abundance of P-glycoprotein (Pgp) (**c**) and receptor for advanced end glycation end products (RAGE) (**d**) compared to β-actin determined by immunoblotting of brain microvessels from 9 month old *APP$^{sw/0}$ Pdgfrβ$^{+/+}$* and *APP$^{sw/0}$*; *Pdgfrβ$^{+/-}$* littermates. **e-f**, Relative abundance of insulin-degrading enzyme (IDE) (**d**) and neprilysin (NEP) (**e**) compared to β-actin determined by immunoblotting in forebrain homogenates from 9 month old *APP$^{sw/0}$*; *Pdgfrβ$^{+/+}$* and *APP$^{sw/0}$*; *Pdgfrβ$^{+/-}$* littermates. In **a-f**, mean ± s.e.m., n=4 mice per group. NS, non-significant by Student's t-test. **g-h**, Relative abundance of PDGFRβ compared to β-actin in brain microvessels derived from 9 month old *Pdgfrβ$^{+/+}$, Pdgfrβ$^{+/-}$*, *APP$^{sw/0}$*; *Pdgfrβ$^{+/+}$* and *APP$^{sw/0}$*; *Pdgfrβ$^{+/-}$* littermates. In **h**, mean ± s.e.m., n=3 mice per group. NS, non-significant by ANOVA followed by Tukey's posthoc tests.

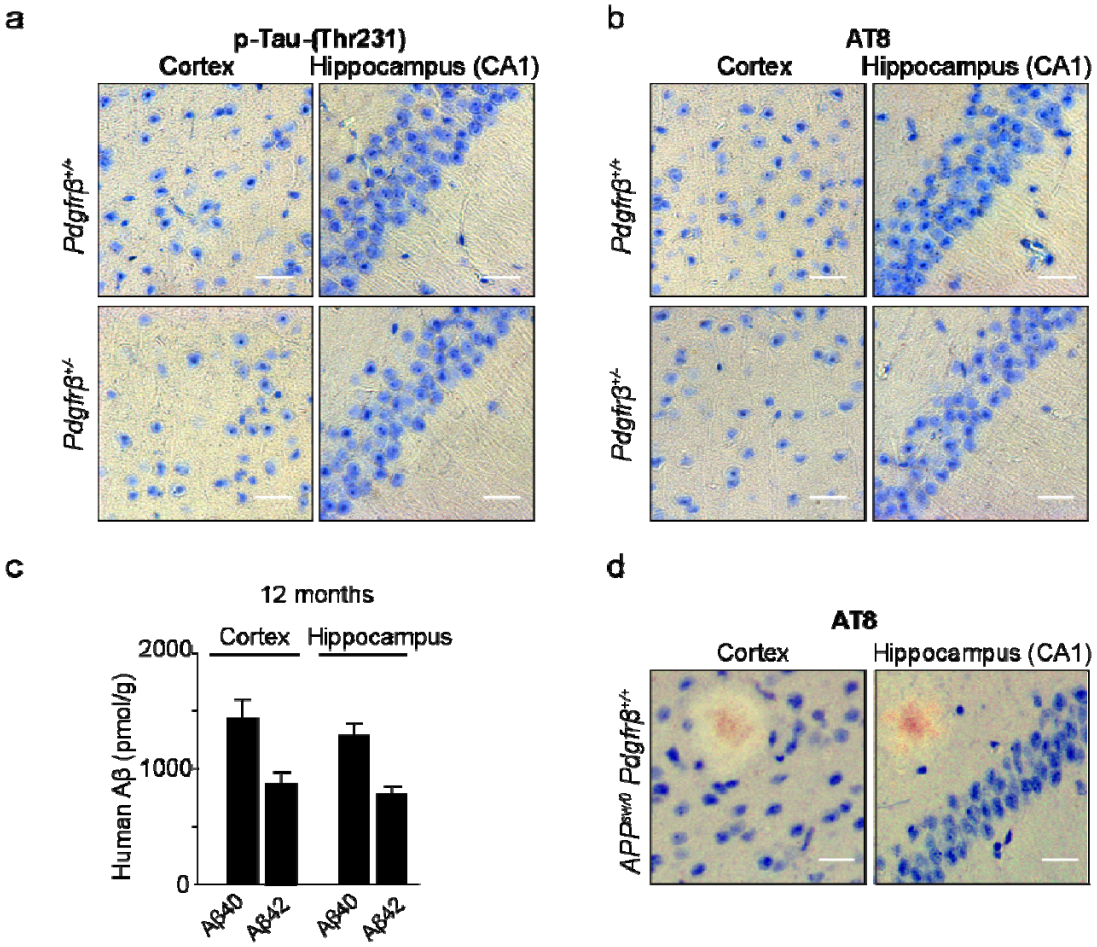

Supplementary Figure S3. Absence of p-tau in *Pdgfrβ*$^{+/-}$ mice and *APP*$^{sw/0}$ *Pdgfrβ*$^{+/+}$ mice. a-b, Representative cortex and hippocampus sections stained with antibodies against p-tau (Thr231) (**a**) and p-tau (Ser202/Thr205, AT8) (**b**) from 9 month old *Pdgfrβ*$^{+/+}$ and *Pdgfrβ*$^{+/-}$ mice. Scale bar, 25 µm. **c**, Human Aβ40 and Aβ42 levels in the cortex and hippocampus in 12 month old *APP*$^{sw/0}$; *Pdgfrβ*$^{+/}$ mice. Mean ± s.e.m., n=6 mice per group. **d**, Representative cortex and hippocampus sections stained against p-tau (Ser202/Thr205, AT8) in 12 month old *APP*$^{sw/0}$; *Pdgfrβ*$^{+/+}$ mouse. Scale bar, 25 µm. In **a**, **b** and **d**, images are representative findings from 6 mice per group.

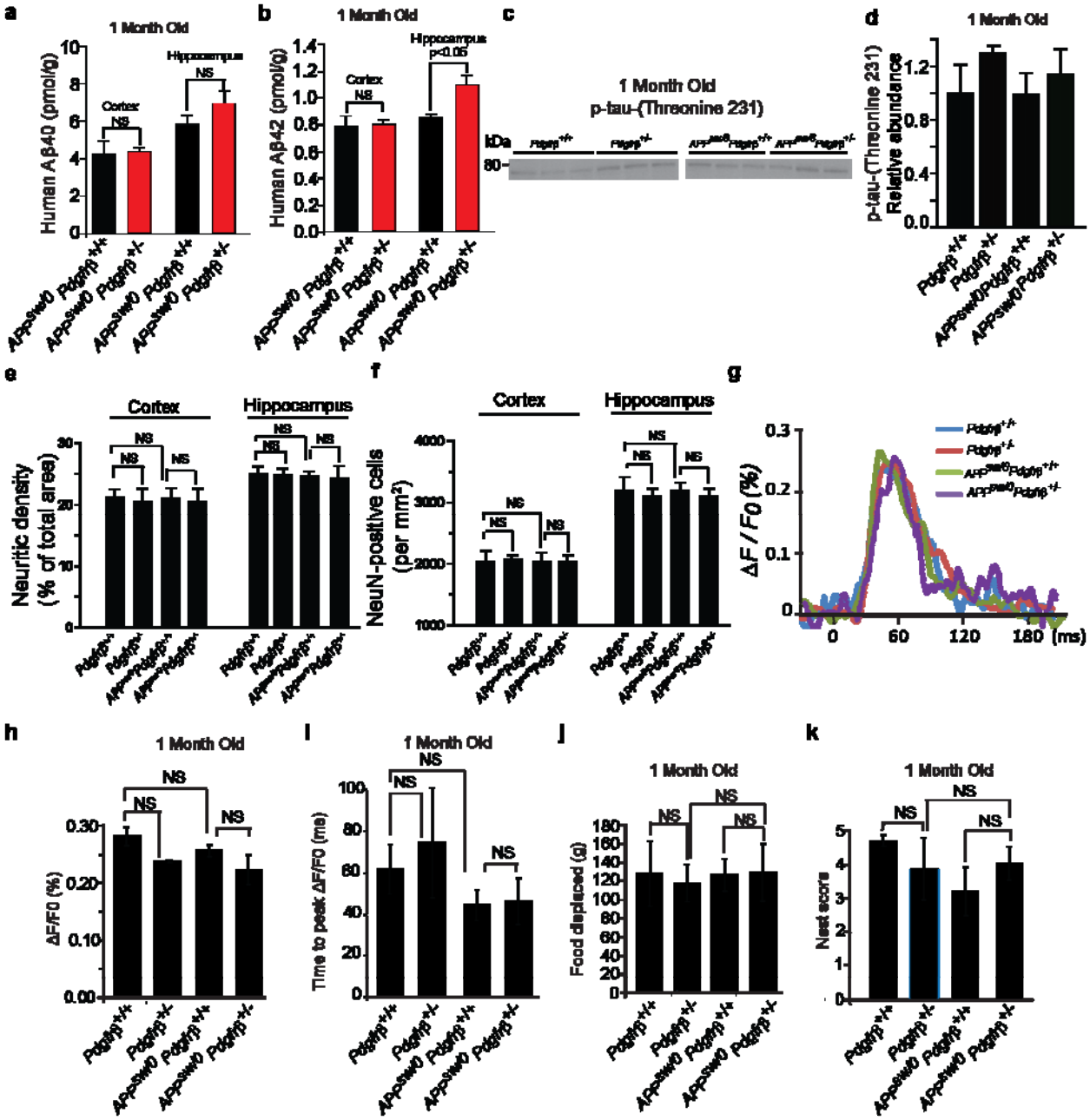

Supplementary Figure S4. Absence of structural and molecular pathology in young pericyte-deficient *APP$^{sw/0}$* mice. a-b, Human Aβ40 and Aβ42 levels in the cortex and hippocampus of 1 month old *APP$^{sw/0}$*; *Pdgfrβ$^{+/+}$* and *APP$^{sw/0}$*; *Pdgfrβ$^{+/-}$* mice. **c-d,** p-tau (Thr231) western blot in forebrain homogenates (**c**) and quantification of p-tau levels relative to total tau (**d**) in 1-2 month old *Pdgfrβ$^{+/+}$*, *Pdgfrβ$^{+/-}$*, *APP$^{sw/0}$*; *Pdgfrβ$^{+/+}$* and *APP$^{sw/0}$*; *Pdgfrβ$^{+/-}$* mice. **e-f**, Quantification of SMI311-positive neurofilaments (**e**) and NeuN-positive neurons (**f**) in the cortex of 9 month old *Pdgfrβ$^{+/+}$*, *Pdgfrβ$^{+/-}$*, *APP$^{sw/0}$*; *Pdgfrβ$^{+/+}$* and *APP$^{sw/0}$*; *Pdgfrβ$^{+/-}$* mice. **g-i**, Representative time-lapse-imaging profile analysis of VSD signal response (**g**), peak amplitude (**h**) and time-to-peak (**i**) in fluorescent VSD signal in the hind-limb somatosensory cortex after stimulation in 1-2 month old *Pdgfrβ$^{+/+}$*, *Pdgfrβ$^{+/-}$*, *APP$^{sw/0}$*; *Pdgfrβ$^{+/+}$* and *APP$^{sw/0}$*; *Pdgfrβ$^{+/-}$* mice.

j-l, Burrowing (**j**), nest construction (**k**) and novel object location (**l**) in 1-2 month old *Pdgfrβ*$^{+/+}$, *Pdgfrβ*$^{+/-}$, *APP*$^{sw/0}$; *Pdgfrβ*$^{+/+}$ and *APP*$^{sw/0}$; *Pdgfrβ*$^{+/-}$ mice. In **a**, **b**, **e**, **f**, **h** and **i**, and in **j** and **k**, mean ± s.e.m., n=5 mice per group. In **d**, mean ± s.e.m., n=3 mice per group. NS, non-significant by ANOVA followed by Tukey's posthoc tests.

Supplementary Figure S5. Full scans of western blots.

Figure 4f APP

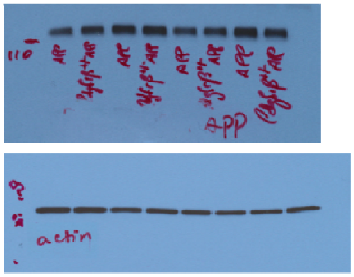

Figure 9a IgG

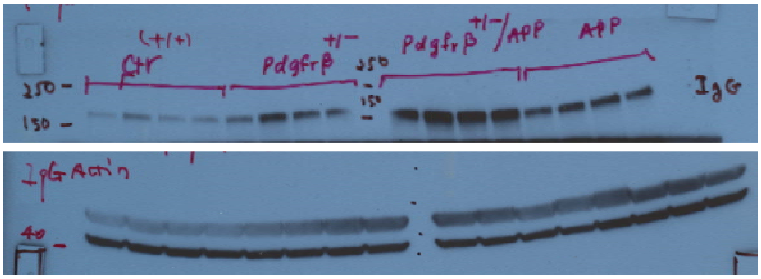

Supplementary Figure S.2a LRP-85

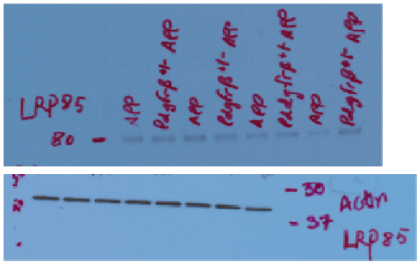

Supplementary Figure S.2b LRP85

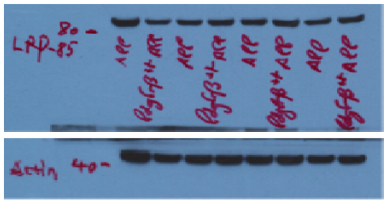

Supplementary Figure S.2c Pgp

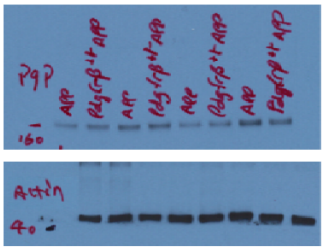

Supplementary Figure S.2d RAGE

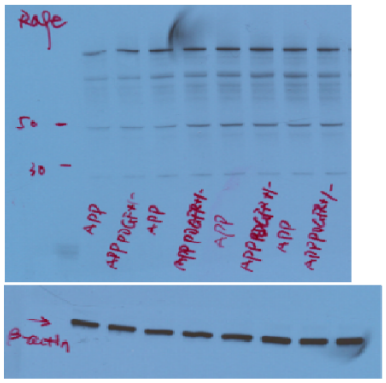

Supplementary Figure S.2e IDE

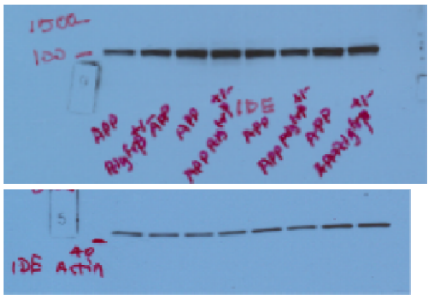

Supplementary Figure S.2f Neprilysin

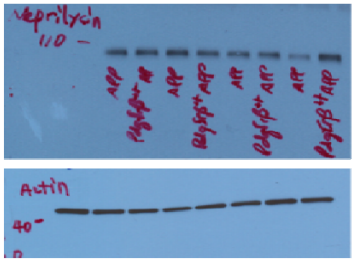

Supplementary Figure S.2g PDGFRβ

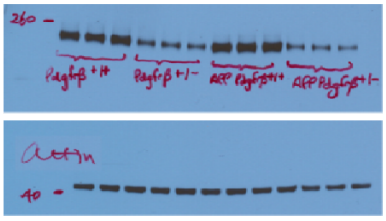

Supplementary Figure S.4c p-tau